Characteristics of Single- and Double-Layer Microstrip Square-Ring Antennas

Pedram Moosavi Bafrooei, *Student Member, IEEE,* and Lotfollah Shafai, *Fellow, IEEE*

***Abstract*— A method for miniaturization of microstrip patch antenna without degrading its radiation characteristics is investigated. It involves perforating the patch to form a microstrip square-ring antenna, which is investigated numerically and experimentally. The ring geometry introduces additional parameters to the antenna that can be used to control its impedance, resonance frequency, and bandwidth. For a single square ring increasing the size of perforation increases its input impedance, but decreases the resonance frequency and bandwidth. It has a small effect on directivity of the antenna. To match the antenna to a transmission line and also enhance its bandwidth, the ring is stacked by a square patch or another square ring. The computed results are compared with experimental data and again good agreement is obtained.**

***Index Terms*—Microstrip antennas, ring, stacked.**

I. Introduction

THE rectangular patch is the most commonly used microstrip antenna, [1] and is characterized by its length and width. Its far-field radiation pattern, losses, quality factor, input impedance, and other electrical parameter are well documented and reported in [2]–[4]. Another configuration is the circular patch antenna and its geometry is characterized by a single parameter, namely, the radius. The expressions for its electrical characteristics are also studied in literature and reported by Bahl and Baharita [5] and Shafai and Antoszkrewicz [6].

The annular ring was first studied by Bergman and Schultz [7] as a traveling wave antenna. It has also been used as a resonator [8], [9] and as a radiator in medical applications [10]. Its resonant behavior is studied by Mink and Christodoulou [11], [12]. It was found that for the ring resonator, the resonant frequency of the lowest order mode can be much lower than that of the circular disc of approximately the same size. There are other features also associated with this antenna. The separation of the modes can be controlled by the ratio of its outer to inner radii. It is also found that when operating in one of the higher order broadside modes, i.e., TM_{12}, the impedance bandwidth becomes several times larger than that achievable in other patch antennas of comparable dielectric thickness. It is possible to combine the annular ring with a second microstrip element, such as a circular disc within its central aperture, to form a compact dual band antenna system [11]. Larger bandwidths can also be obtained using stacked microstrip patches [13]–[15], and multilayer ones [16], revealing interesting features.

Manuscript received November 6, 1997; revised April 18, 1998.

The authors are with the Department of Electrical and Computer Engineering, University of Manitoba, Winnipeg, Manitoba, R3T 5V6 Canada.

Publisher Item Identifier S 0018-926X(99)08844-4.

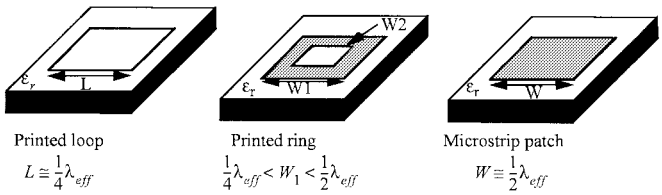

Fig. 1. Geometry of printed loop, ring, and microstrip patch antennas.

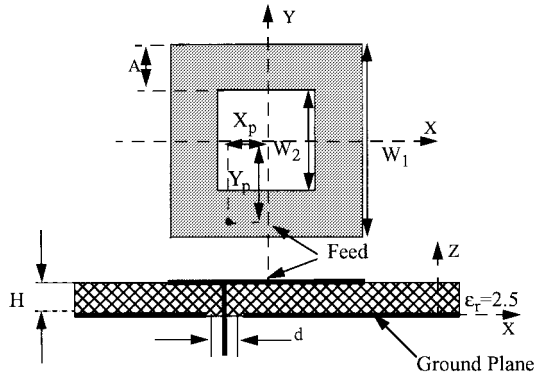

Fig. 2. Microstrip square-ring configuration.

A novel structure that has not been studied well yet is the square-ring patch, which is geometrically an intermediate configuration between a printed loop and solid patch (see Fig. 1) [17]. The intermediate configuration is similar to the patch, except its central conducting portion of width $\mathbf{W_2}$ is removed. This width $\mathbf{W_2}$ provides a new parameter to control its resonance and impedance.

II. Characteristic of Single-Layer Microstrip Square Ring Antennas

The printed ring antenna is similar to a solid patch except that its central conducting portion $\mathbf{W_2}$ is removed. In order to study the characteristics of a square-ring resonator, a solid patch with $\mathbf{W_1} = 30$ mm, dielectric substrate relative permittivity $\varepsilon_r = 2.5$ and thickness $H = 0.8, 1.59, 3.18$ mm is considered. The ground plane is assumed infinite and the patch is fed coaxially at $X_p = 0$ mm, $Y_p = -13$ mm with a probe diameter of $d = 1.27$ mm (Fig. 2). Extensive computations are carried out to obtain the characteristics of the resonator.

A. Resonance Frequency

The resonance frequency of the solid patch for $h = 1.59$ mm and $\mathbf{W_1} = 30$ mm is 3.041 GHz. By increasingly removing the central conducting portion, the resonance frequency decreases, and make it possible to achieve the resonance frequency with

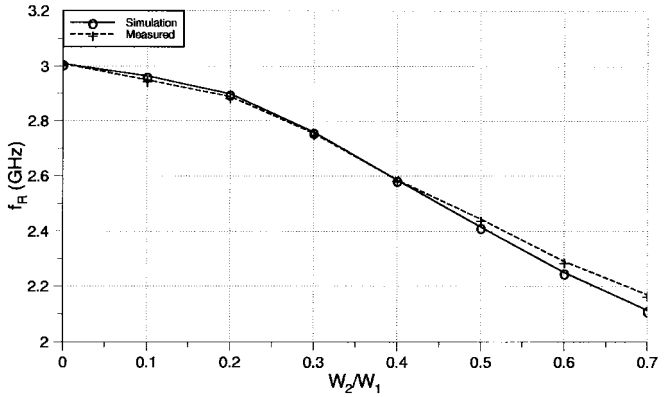

Fig. 3. Measured and calculated resonance frequency variation with W_2, $W_1 = 30$ mm $\varepsilon_r = 2.5, h = 1.59$ mm.

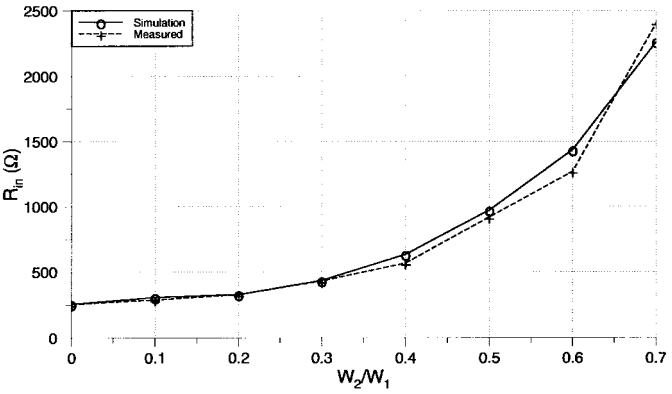

Fig. 4. Measured and calculated input impedance variation with W_2/W_1, $W_1 = 30$ mm, $\varepsilon_r = 2.5$, $h = 1.59$ mm.

a smaller ring size. For instance, when $\mathbf{W_2/W_1} = 0.7$ or $\mathbf{W_2} = 21$ mm the resonance frequency is 2.147 GHz, which is 70% of the patch resonance frequency. This resonance frequency corresponds to a patch having larger size of 43 mm. The simulation and measurement results for different ring sizes are shown in Fig. 3. The resonance frequency f_r is predicted very well for all values of $\mathbf{W}_2$.

The effect of various substrate thicknesses on the resonance frequency is also investigated. The resonance frequency of a solid patch increases slightly by decreasing the thickness of substrate. However, this is not true for the ring. As the size of perforation is increased the resonance frequency reduces, but the rate of reduction is faster for a thinner substrate. As an example, for $\mathbf{W_2/W_1} = 0.7$ the resonance frequency was found to be 2.084 GHz for $h = 0.8$ mm, which is 67% of its initial value of 3.111 GHz for a solid patch. Comparing this result to that of $h = 1.59$ mm in Fig. 3, one observes that the resonance frequency has further decreased by 3% [18].

B. Input Impedance

The calculated and measured values of the input impedance for a coaxially fed square-ring resonator with $\varepsilon_r = 2.5$ and $h = 1.59$ mm are shown in Fig. 4. When $\mathbf{W_2}$ is increased the input impedance at resonance frequency for the ring, i.e., $R_{\mathbf{in}}$, increases.

The input impedance at resonance frequency is also dependent on the substrate thickness. It increases by decreasing

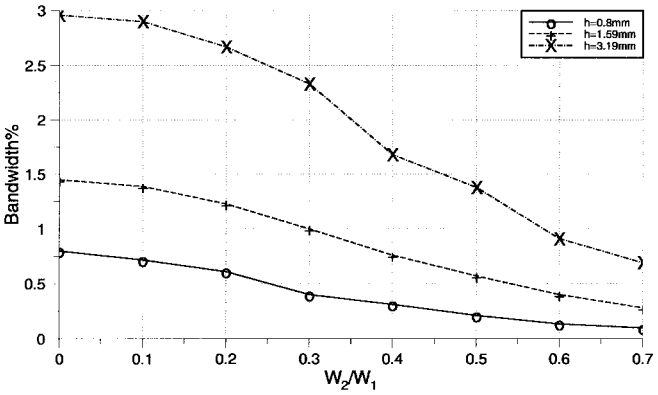

Fig. 5. Calculated bandwidth for various substrate thicknesses $W_1 = 30$ mm, $\varepsilon_r = 2.5$.

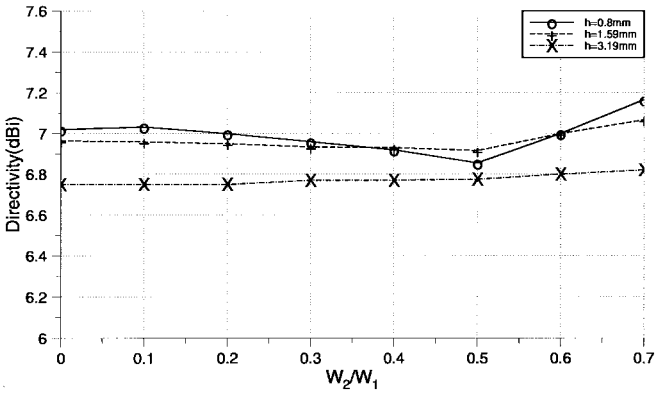

Fig. 6. Calculated directivities for several substrate thicknesses $W_1 = 30$ mm, $\varepsilon_r = 2.5$.

h. For all cases, when the ring width decreases, i.e., $\mathbf{W_2}$, is increased, the input impedance increases rapidly to few thousands Ω and becomes difficult to feed the antenna with a 50 Ω transmission line.

C. Impedance Bandwidth

The ring resonator bandwidths for different values of h are shown in Fig. 5. As expected the bandwidth for the patch increases by increasing the substrate thickness. But, as the size of its perforation is increased, the bandwidth reduces rapidly. The rate of this reduction is increased by decreasing h. For $h = 3.19$ mm, the bandwidth reduces from 2.96% for a solid patch to 0.69% for $\mathbf{W_2/W_1} = 0.7$, a reduction of about 76%. The reduction for $h = 1.69$ mm is 80.7% and for $h = 0.8$ mm it is 88%. Since the size reductions are about 37%, it will be clear that the bandwidth decreases at a faster rate.

D. Directivity

The ring directivity as a function of $\mathbf{W_2/W_1}$ for three substrate heights is illustrated in Fig. 6. The dielectric thickness has small effect on the directivity, which is similar to the solid patch. Similarly, the perforation size $\mathbf{W_2}$ has a negligible effect on the directivity. This is a surprising result since by increasing $\mathbf{W_2}$ the resonance frequency decreases, i.e., the wavelength increases and the antenna size in wavelength decreases. Thus, since the antenna physical area has remained constant, its directivity should decrease accordingly

$$D_0 = 4\pi \frac{A_{em}}{\lambda^2}. \tag{1}$$

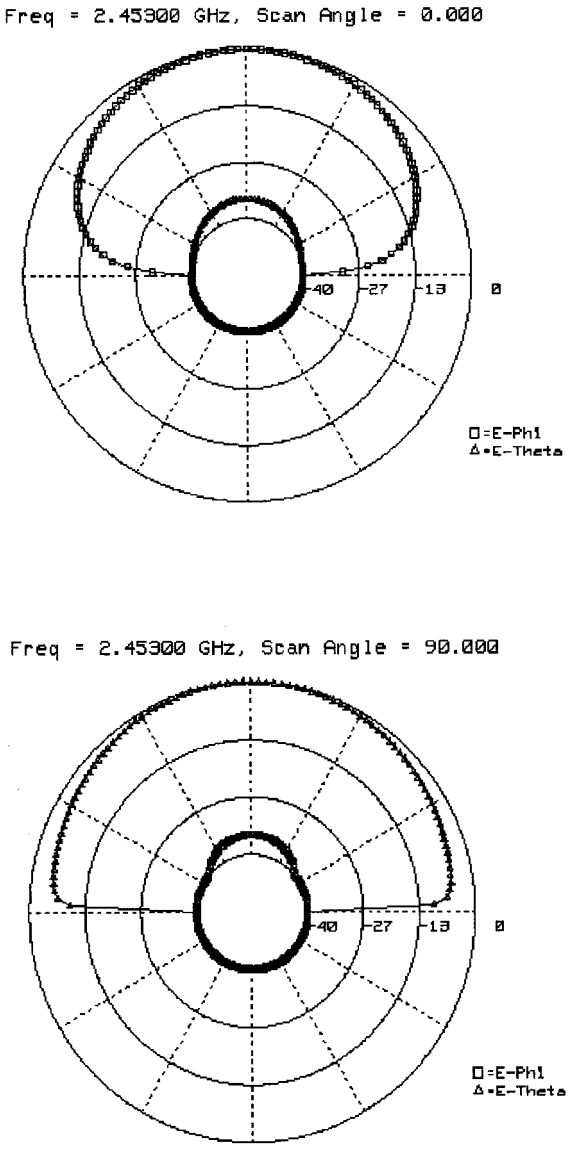

Fig. 7. H- and E-plane radiation patterns for $h = 1.59$ mm and $W_2/W_1 = 0.5$, $W_1 = 30$ mm, $\varepsilon_r = 2.5$.

However, Fig. 6 shows that the antenna directivity is independent of the perforation size and may even increase with it. This indicates that the ring effective aperture A_{em} must be increasing by increasing its perforation size $\mathbf{W_2}$ to compensate for the increase in the wavelength.

E. Radiation Patterns

The E- and H-plane radiation patterns of the ring with $\mathbf{W_2/W_1} = 0.5$ in the principal $\phi = 0$ and $\phi = 90$ planes, are shown in Fig. 7. They are similar to those of a solid patch and show negligible cross polarization. The 3-dB beamwidth for the H-plane is about 81° and for the E-plane is 110° and are not sensitive to the substrate height or the perforation size $\mathbf{W_2}$.

The influence of $\mathbf{W_2/W_1}$ on the cross polarization in the H-plane is shown in Fig. 8. The effect is negligible and within the computational errors. However, its variation increases by decreasing H—the substrate thickness. These values are not the maximum cross polarization, which occurs in the $\phi = 45$ plane.

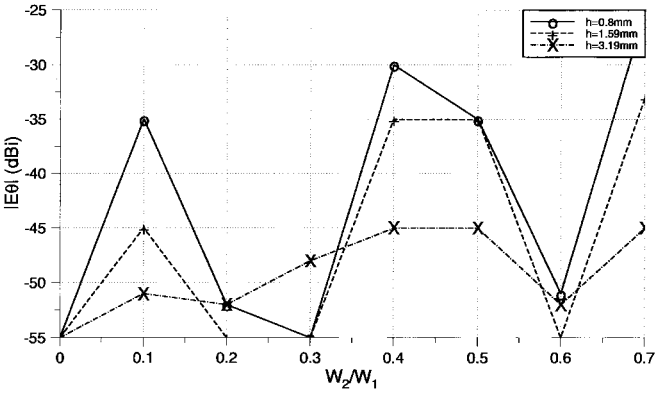

Fig. 8. Normalized cross polarization in the H-plane, for ring antenna with $W_1 = 30$ mm, $\varepsilon_r = 2.5$.

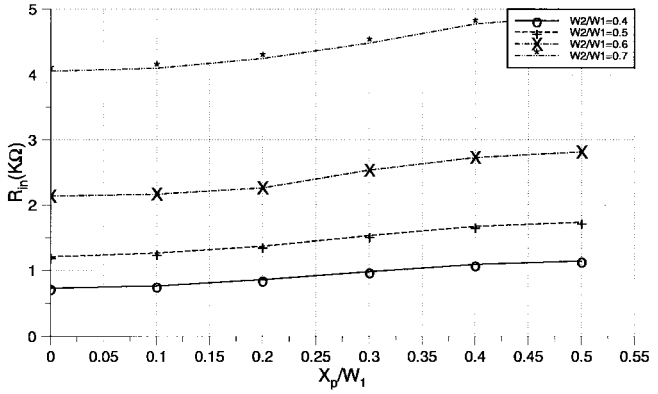

Fig. 9. Input resistance at resonance versus probe position for different ring sizes $Y_p = -13$ mm, $W_1 = 30$ mm, $\varepsilon_r = 2.5, h = 1.5$ mm.

F. Effect of Moving Feed Probe

The influence of the perforation size $\mathbf{W_2}$ to modify a ring width A on its electrical parameters was investigated in the previous sections. In particular, it was found that the input impedance increases by increasing $\mathbf{W_2}$. In all above cases, however, the feed probe was located near the outer edge of the ring on its symmetry axis, i.e., the y axis. Since in a solid patch the input impedance depends on the feed location, it is constructive to investigate this effect also for the ring antenna by moving the feed along both x and y axes.

To investigate the effect of moving the feed along the x axis, it was maintained near the outer edge, i.e., $\mathbf{Y_p/W1} = 0.44$ and $\mathbf{X_p}$ increased from 0 to 0.5 $\mathbf{W_1}$ (Fig. 2). As for a solid patch, moving the feed toward the corner did not indicate a noticable change in the resonance frequency, but increased the cross polarization. It also increased the input impedance as shown in Fig. 9. The input impedance increases, regardless of $\mathbf{W_2}$, but the rate of increase seems increases by increasing $\mathbf{X_p}$.

The effect of moving the probe along the symmetric y axis, i.e., $\mathbf{X_p} = 0$, toward its inner edge was also investigated. Again, it was found that this displacement had no influence on the resonance frequency, but the input impedance decreased. Also, because of the symmetry in this case, no variation in the radiation patterns was observed. The input impedance for different probe locations and different ring sizes are shown in Fig. 10. For this inner location of the feed the

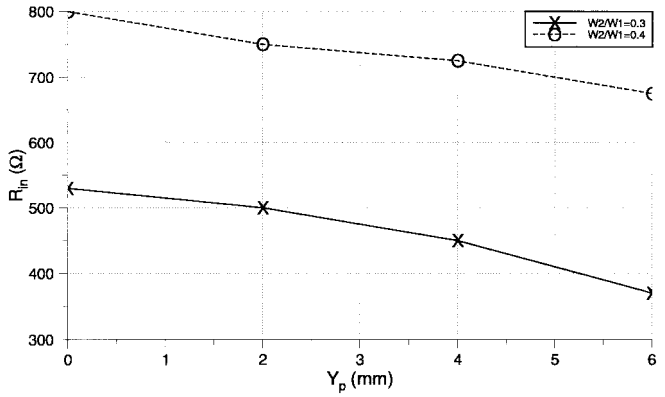

Fig. 10. Input resistance at resonance versus probe position in y direction, $X_p = 0$ mm, $W_1 = 30$ mm, $\varepsilon_r = 2.5$.

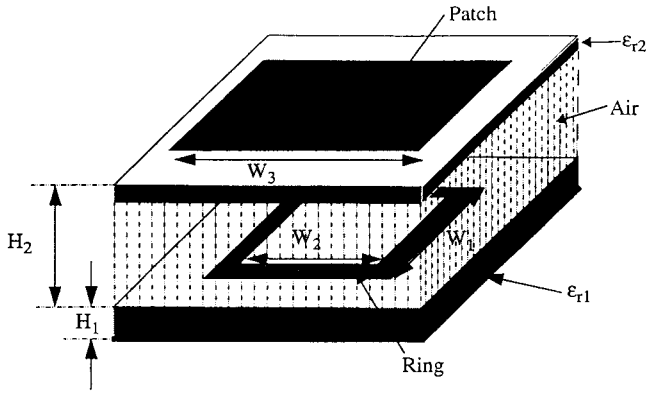

Fig. 11. Configuration of a stacked ring-patch antenna.

reduction in the input impedance can help with impedance matching. In addition, because the feed is located close to the perforated area, it is possible to place the feeding network or an monolithic microwave integrated circuit (MMIC) at the center of the ring. This may be a useful feature in integrating the antenna with its electronics or placing beamforming network components within the array elements.

III. Stacked Ring Reesonators for Bandwidth Enhancment

It was observed in Section II that the input impedance of a microstrip square ring at the resonance frequency increases rapidly as its width decreases, i.e., $\mathbf{W_2}$ increases. Thus, it becomes impractical to match the ring to a 50 Ω transmission line using a stub or quarter-wave line. Also it becomes very narrow band. These disadvantages are serious and prevent its use in practical applications. Thus, efforts have been made in this study to overcome these limitations.

Increased bandwidth and matched impedance can be obtained in a variety of ways by using parasitically coupled elements to produce a double-tuned resonance configuration. A convenient approach uses stacked resonators with adjacent resonance frequencies. Naturally, the antenna performance will depend on its parameters, which are the heights and dielectric constants of the two substrates. Thus, by tuning these parameters it should possible to enhance the bandwidth and also to match the antenna to low impedances. The result of this study are presented below.

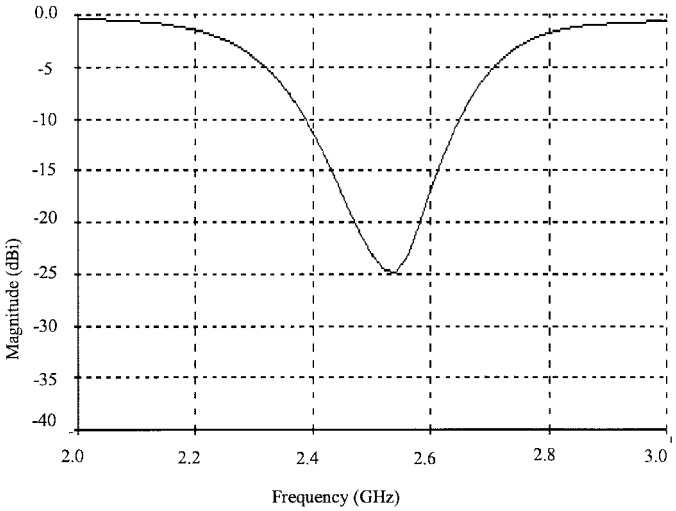

Fig. 12. Computed return loss of the stacked ring-patch configuration $W_2/W_1 = 15/30$, $W_3 = 47$ mm, $H_1 = 1.6$ mm, $H_2 = 5$ mm, $\varepsilon_{r1} = 2.5$, $\varepsilon_{r2} = 1.05$.

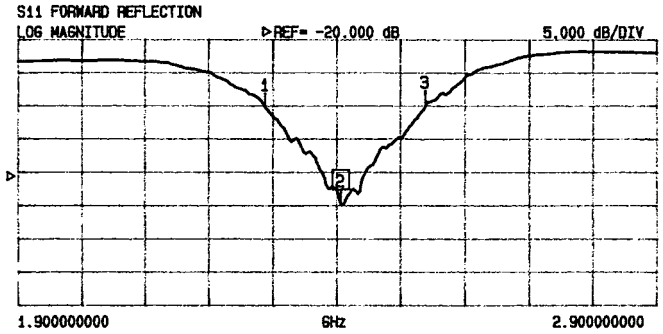

Fig. 13. Measured return loss of the stacked patch configuration of Fig. 12.

A. Stacked Ring Patch

First, we consider stacking a patch over a ring (Fig. 11). A design was completed with $\varepsilon_{r1} = 2.5$, $H_1 = 1.5$ mm, $W_1 = 30$ mm, $W_2 = 15$ mm, $\varepsilon_{r2} = 1.05$ (foam) $H_2 = 5$ mm, $W_3 = 47$ mm, $d = 1.27$ mm, $X_p = 0$ mm, and $Y_p = -13$ mm (X_p, Y_p are shown in Fig. 2 and simulated in Fig. 3).

One sample was fabricated and tested by "Wiltron 37269A" network analyzer and its mid-band radiation pattern measured in the "anechoic chamber." They are shown in Figs. 12–14.

Excellent agreement between the theory and experiment is observed for a coaxially fed antenna. In numerical computation, the cell size for the top layer is $0.01\lambda_0$ and for the bottom layer $0.034\lambda_0$, where λ_0 is the wavelength at mid-band frequency of 2.5 GHz.

Figs. 12 and 13 show the computed $S11$ with a 50-Ω line and its corresponding measured results. They agree well. From Fig. 12, the resulting bandwidth for a VSWR < 2 is about 10.5%, which shows a significant improvement over those of a single ring antenna.

For the ring-patch antenna the 3-dB beamwidths are (for a ground plane size $= 0.83\lambda_0$) 65° (E-plane) and 75° (H-plane), having a difference of 10°. Fig. 14 gives the mid-band measured radiation patterns in both E and H planes. The measured gain of this structure is 8.7 dBi. Note that the measured radiation patterns are for a finite ground plane,

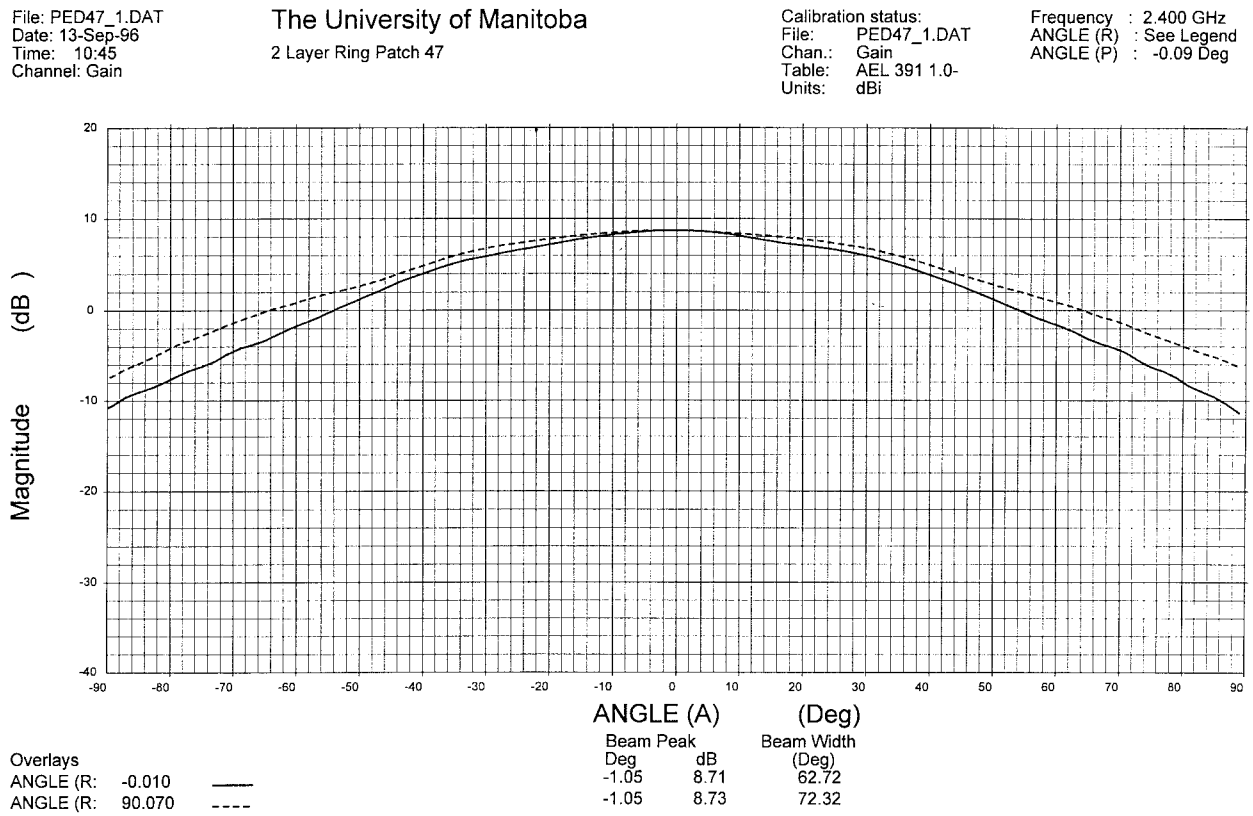

Fig. 14. Measured E- and H-plane radiation patterns for ring-patch antenna of Fig. 12.

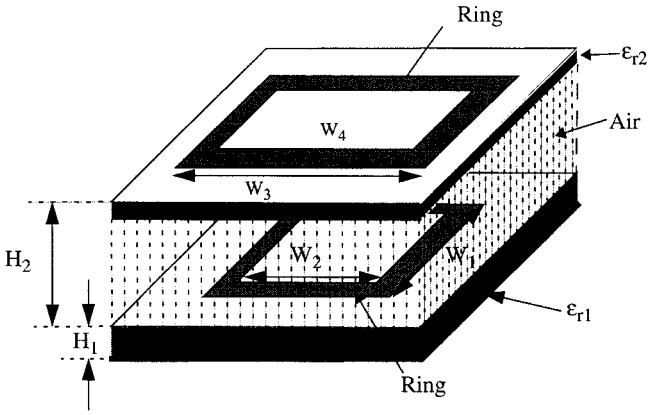

Fig. 15. Configuration of stacked ring-ring antenna.

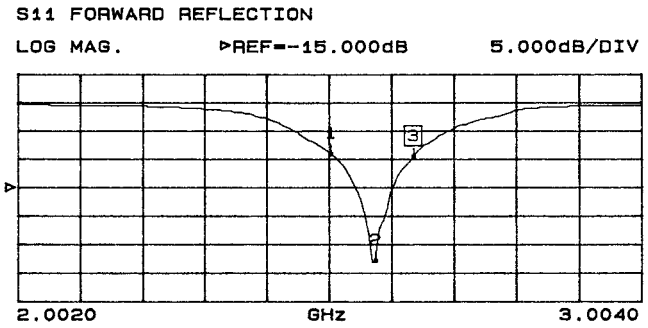

Fig. 16. Measured return loss of the stacked rings, $W_2/W_1 = 14/30$, $W_4/W_3 = 22/36$, $H_1 = 1.6$ mm, $H_2 = 5$ mm, $\varepsilon_{r1} = 2.5$, $\varepsilon_{r2} = 1.05$.

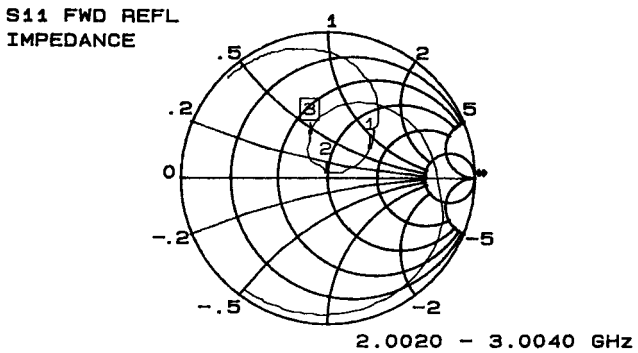

Fig. 17. Measured input impedance of stacked ring antenna of Fig. 16.

but the computed ones for an infinite ground plane. Some deviations in gain and bandwidths of the principal plane patterns are expected.

B. Stacked Ring Ring

For stacking, it is possible to use another ring instead of the patch to not only enhance the bandwidth but also to reduce the total size of the antenna (Fig. 15). The geometry of the antenna is shown in Fig. 4. It consists of a two layer ring with $\varepsilon_{r1} = 2.5$, $H_1 = 1.5$ mm, $W_1 = 30$ mm, $W_2 = 14$ mm, $\varepsilon_{r2} = 1.05$ (foam) $H_2 = 5$ mm, $W_3 = 36$ mm, $W_4 = 22$ mm, $d = 1.27$ mm, $X_p = 0$ mm, and $Y_p = -13$ mm, (X_p, Y_p are shown in Fig. 2) which was designed and simulated.

One sample was fabricated and tested by "HP 8722C" network analyzer and its mid-band radiation patterns measured in the "anechoic chamber." They are shown in Figs. 16–18. Good agreement between the theory and experiment is observed for a coaxially fed antenna.

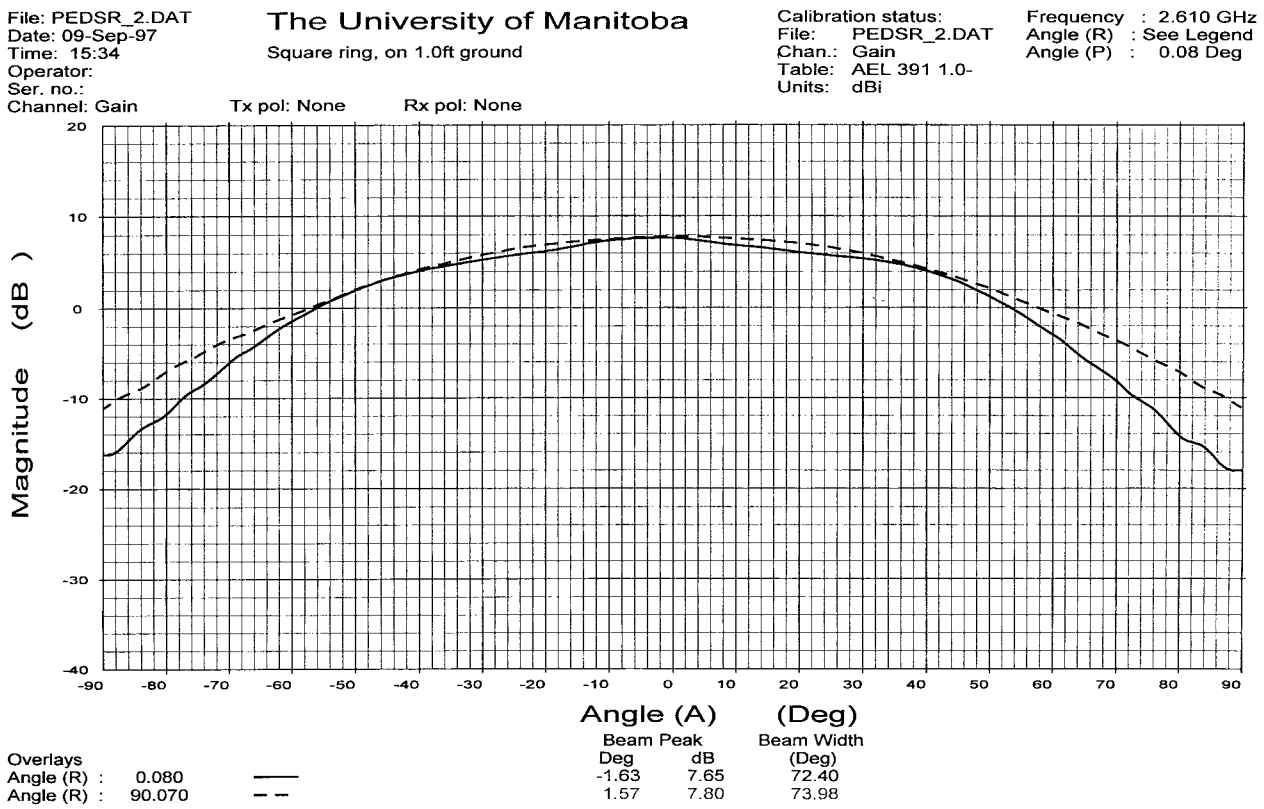

Fig. 18. Measured E- and H-plane radiation pattern with cross polarization for Fig. 16.

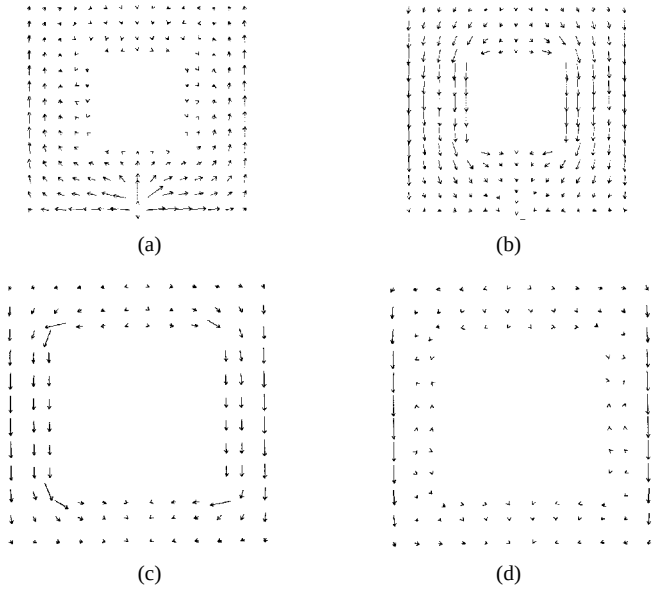

Fig. 19. Real and imaginary normalized surface current components. (a) Real current component on lower ring $I_{R\max} = 0.005\,615$. (b) Imaginary current component on lower ring $I_{I\max} = 0.009\,578$. (c) Real current component on upper ring, $I_{R\max} = 0.019\,038$. (d) Imaginary current component on upper ring $I_{I\max} = 0.002\,046$.

In numerical computation, the cell size for the top layer is $0.026\lambda_0$ and for the bottom layer $0.017\lambda_0$, where λ_0 is the wavelength at mid-band frequency of 2.6 GHz. From Figs. 16 and 17, the resulting bandwidths, for a VSWR < 2 were about 6.4% experimentally and 5.4% by simulation. They are smaller than that of the previous example of ring-patch antenna, i.e., 10.5%, but still considerably better than a single-layer ring.

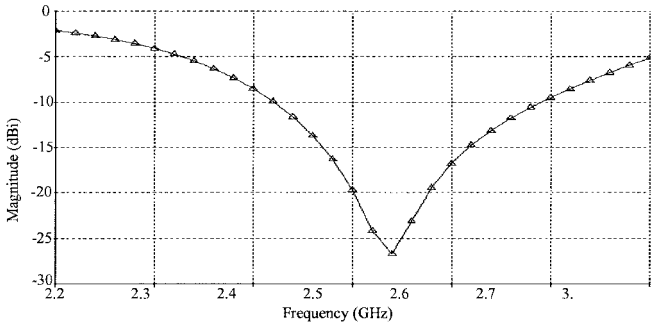

Fig. 20. Return loss for a stacked ring-ring antenna with $H_1 = 3.2$ mm.

For the ring-ring antenna the 3-dB beamwidths are 61° (E-plane) and 74° (H-plane), having a difference of 13°. The gain of this structure was found to be 8.0 dBi. The current distributions on the surfaces of the rings were also computed and shown in Fig. 19. The current intensity is high and undergoes rapid variation at corners.

C. Effect of Changing H_1

To consider the effect of changing the lower substrate thickness, a practical case was simulated. In this case, the lower substrate thickness of the previous example with $\varepsilon_r = 2.5$ was increased to 3.2 mm. The other parameters are as follows: $W_1 = 30$ mm, $W_2 = 15$ mm, $\varepsilon_{r2} = 1.05$ (foam), $H_2 = 5$ mm, $W_3 = 42$ mm, $W_4 = 14$ mm, $d = 1.27$ mm, $X_p = 0$ mm, and $Y_p = -13$ mm.

From Fig. 20, the resulting bandwidth for a VSWR < 2, is about 11% by simulation, which has doubled from the previous case, naturally, due to increasing the lower substrate thickness

H_1. For this case, the 3-dB beamwidths are 72° (E-plane) and 74° (H-plane), having a difference of 2°. The gain of this antenna is 8.2 dBi.

IV. Conclusion

A study was carried out to determine the effects of removing central conducting portion of the microstrip square patch antennas on their radiation characteristics. A numerical method based on a full wave approach using mixed potential integral formulation in conjunction with the method of moment was utilized. In this method, the resonance frequency, input impedance, current distribution, and radiation pattern are computed accurately. Adequate measurements were performed to confirm the computed results.

Perforating the square patch to become a square ring has significant effect on its resonance frequency and input impedance. The resonance frequency decreases by increasing the size of perforation and this reduction is faster for thinner substrates. By decreasing the ring width, the input impedance increases rapidly and also the bandwidth reduces at a faster rate than the size reduction. Inspite of reduction in the antenna size, the directivity remains constant and does not change by modifying substrate thickness. Also, the perforation on conducting portion causes current discontinuities and, therefore, results in rapid variation in its magnitude and direction.

For matching the square-ring antenna to any impedance and also enhancing its bandwidth stacking technique was used. In this method, both a patch and another ring were used. The bandwidth and also input impedance of these structures were tuned by changing the substrate thickness and permittivity. The gain of this antenna was found to be independent of the ring sizes.

References

[1] J. Q. Howell, "Microstrip antennas," *IEEE Trans. Antennas Propagat.*, vol. AP-23, pp. 90–93, Jan. 1975.

[2] J. R. James, P. S. Hall, and C. Woods, *Microstrip Antenna Theory and Design*. London, U.K.: Peter Peregrinus, 1981.

[3] Y. T. Lo, D. Solomon, and W. F. Richards, "Theory and experiment on microstrip antennas," *IEEE Trans. Antennas Propagat.*, vol. AP-27, pp. 137–145, Mar. 1979.

[4] W. F. Richards, Y. T. Lo, and D. D. Harrison, "An improved theory for microstrip antennas and applications," *IEEE Trans. Antennas Propagat.*, vol. AP-29, pp. 38–46, Jan. 1981.

[5] I. J. Bahl and P. Bhartia, *Microstrip Antennas*. Dedham, MA: Artech House, 1982.

[6] K. Antoskiewicz and L. Shafai, "Impedance characteristics of circular microstrip patches," *IEEE Trans. Antennas Propagat.*, vol. 38, pp. 942–946, June 1990.

[7] W. J. Bergman and F. V. Schultz, "The circular traveling-wave antenna," *IRE Int. Conv. Rec.*, vol. 3, pt. 1, pp. 40–50, 1955.

[8] Y. S. Wu and F. J. Rosenbaum, "Mode for microstrip ring resonator," *IEEE Trans. Microwave Theory Tech.*, vol. MTT-21, p. 487, July 1973.

[9] S. Pintzos and R. Pregla, "A simple method for computing the resonant frequencies of microstrip ring resonator," *IEEE Trans. Microwave Theory Tech.*, vol. MTT-26, p. 809, Oct. 1978.

[10] I. J. Bahl, S. S. Stuchly, and M. A. Stuchly, "A new microstrip radiator for medical application," *IEEE Trans. Microwave Theory Tech.*, vol. MTT-28, p. 1464, pp. 1464–1468, Dec. 1980.

[11] J. W. Mink, " Cicular ring microstrip antenna elements," *IEEE Trans. AP-S Int. Symp. Dig.*, Laval, Quebec, Canada, June , 1980, pp. 605–608.

[12] G. Tagle and C. G. Christodoulou, "Extended cavity model analysis of stacked ring antennas," *IEEE Trans. Antennas Propagat.*, vol. 45, pp. 1626–1635, Nov. 1997.

[13] S. A. Long and M. D. Walton, "A dual-frequency, stacked circular disc antenna," *IEEE Trans. Antennas Propagat.*, vol. AP-27, pp. 270–276, Mar. 1979.

[14] R. T. Cock and C. G. Christofedoulu, "Design of a two-layer, capasitively coupled, microstrip patch antenna element for broadband applications," *IEEE Trans. AP-S Int. Symp. Dig.*, Blacksburg, VA, June, 1987, pp. 936–939.

[15] F. Croq, "Stacked resonator for bandwidth enhancment, a comparison of two feeding techniques," *Proc. Inst. Elect. Eng.*, vol. 140, pt. H, pp. 303–309, Aug. 1993.

[16] J. P. Damiano, J. Bennegueouche, and A. Papiernik, "Study of multilayer microstrip antennas with radiating elements of various geometry," *Proc. Inst. Elect. Eng.*, vol. 137, pt. H, pp. 163–170, June 1990.

[17] L. Shafai, "Characteristics of printed ring antennas," *Symp. Antenna Technol. Appl. Electromagn.*, Montreal, Canada, Aug. 1996, vol. 96, pp. 379–382.

[18] P. Moosavi, "Characteristic and design of microstrip square ring antennas," M.Sc. thesis, Univ. Manitoba, Canada, Aug. 1997.

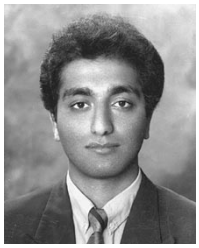

Pedram Moosavi Bafrooei (S'94) was born in 1972, Tehran, Iran. He received the B.Sc. degree (communication engineering) from Iran University of Science and Technology (IUST), Tehran, in 1995, and the M.Sc. degree (electrical engineering) from the University of Manitoba, Canada, in 1997. He is currently working toward the Ph.D. degree (electrical engineering) at the University of Manitoba.

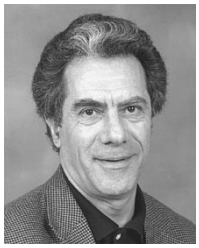

Lotfollah Shafai (S'67–M'69–SM'75–F'88) received the B.Sc. degree from the University of Tehran, Iran, in 1963, and the M.Sc. and Ph.D. degrees from the Faculty of Applied Sciences and Engineering, University of Toronto, ON, Canada, in 1966 and 1969, respectively, all in electrical engineering.

In November 1969, he joined the Department of Electrical and Computer Engineering, University of Manitoba as a Sessional Lecturer. He became an Assistant Professor in 1970, an Associate Professor in 1973, and a Professor in 1979. Since 1975 he has made a special effort to link the university's research to the industrial development by assisting industries in the development of new products or establishing new technologies. To enhance the contact of the University of Manitoba with industry, in 1985 he assisted in establishing "the Institute for Technology Development," and was its Director until 1987, when he became the Head of the Electrical Engineering Department. His assistance to industry was instrumental in establishing an Industrial Research Chair in Applied Electromagnetics at the University of Manitoba in 1989, which he held until July 1994.

Dr. Shafai has been a participant in nearly all Antennas and Propagation Symposia and participates in the review committees. He is a member of URSI Commission B and was its chairman from 1985 to 1988. In 1986 he established the Symposium on Antenna Technology and Applied Electromagnetics (ANTEM) at the University of Manitoba, which is currently held every two years. He has been the recipient of numerous awards. In 1978 his contribution to the design of a small ground station for the Hermus satellite was selected as the 3rd Meritorious Industrial Design. In 1984 he received the Professional Engineers Merit Award and, in 1985, "The Thinker" Award from Canadian Patents and Development Corporation. From the University of Manitoba, he received the "Research Awards" in 1983, 1987, and 1989, the Outreach Award in 1987, and the Sigma Xi Senior Scientist Award in 1989. In 1990 he received the Maxwell Premium Award from the Institute of Electrical Engineers (London) and in 1993 and 1994 he received the Distinguished Achievement Awards from Corporate Higher Education Forum. In 1998 he received the Winnipeg RH Institute Foundation Award for Excellence in Research. In 1998 he was elected a Fellow of the Royal Society of Canada.